AIAA JOURNAL
Vol. 33, No. 11, November 1995

Comparison of High-Resolution Schemes Applied to Flows Containing Strong Shocks

K. Sundar,* V. Sriramulu,† and M. Ramakrishna‡
Indian Institute of Technology, Madras 600 036, India

A comparison of three high-resolution schemes is carried out for a representative two-dimensional problem. Two explicit schemes, namely, the MacCormack scheme and the Strang type operator split scheme, and one implicit scheme, namely, the Beam and Warming scheme, are compared. Harten's modified flux approach is adopted to achieve the high resolution and total variation diminishing property. It is found that a combination of explicit (operator split) and implicit schemes performs best in terms of quality of solution, convergence, and CPU time. Implicit schemes take marginally more time but perform just as well as the combination scheme. Between the explicit schemes, the operator split scheme is better.

Nomenclature

A = Jacobian of flux vector E
a = eigenvalue of matrix A or B
B = Jacobian of flux vector F
c = speed of sound
E = flux vector along x direction
e_t = total internal energy per unit volume
F = flux vector along y direction
g = upwind limiter
J = metric Jacobian
p = pressure of gas
p_{fs} = freestream pressure
p_w = wall pressure
p_0 = stagnation pressure
Q = vector of conservation variables
R = matrix containing the right eigenvectors
T = temperature of gas
U = contravariant velocity component along ξ direction
u = velocity component along x direction
V = contravariant velocity component along η direction
v = velocity component along y direction
α = characteristic variable
β = symmetric limiter
γ = ratio of specific heats of an ideal gas
ρ = density of gas
Φ = explicit TVD dissipation
Ω = implicit TVD dissipation

Introduction

INTEREST in the design of inlets for scramjets and ramjets and hypersonic re-entry vehicles has led to vast improvements in the computation of flowfields with strong shocks. The schemes used previously[1] to simulate such flowfields either produced oscillations in the vicinity of the shock when no artificial dissipation was added or produced smeared shocks when dissipation was added. Although the quality of solution could be improved through proper control of dissipation, it involved empiricism and trial and error procedures. In recent years, many second-order accurate shock capturing finite difference schemes for the computation of Euler equations have been developed. They generate nonoscillatory but sharp approximations to shock and contact discontinuities.[2–4] These methods, although widely different, have the same design principle, namely, all these schemes are total variation diminishing (TVD). Several authors[5–8] have proposed different design principles to achieve TVD and second-order accuracy.

In the present paper the modified flux approach of Harten is adopted. It is a technique to design a second-order accurate scheme starting with a first-order TVD scheme and applying it to a modified flux. The modified flux is chosen so that the scheme is second-order accurate in regions of smoothness and first-order accurate at points of extrema. From the implementation point of view the modified flux approach can be viewed as a three-point central scheme with a "smart" dissipation, wherein there is automatic feedback which controls the amount of numerical dissipation. The advantage is that it can be incorporated into existing computer codes by replacing the classical dissipation with the newer dissipation, which ensures that the overall algorithm behaves as TVD.

Although extensive comparisons for the scalar and one-dimensional schemes have been reported,[9,10] comparisons of performance of TVD schemes in high dimensions have been few.[11] The objective of the present work is to compare the performance of two explicit schemes and an implicit scheme for a representative two-dimensional problem, namely, the blunt body problem. Performance here is characterized by the solution quality, CPU time, and the rate of convergence. The blunt body is chosen as representative since extensive results, both experimental and numerical, are reported. The two explicit schemes chosen are the MacCormack predictor corrector scheme[12] and the Strang type dimensional splitting method.[13] The implicit scheme chosen is the Beam and Warming scheme.[14] These three schemes are chosen in view of their popularity and their extensive use.

A brief description of the algorithms is followed by the explanation of the dissipation, and then the initial and boundary conditions adopted in the present study are described. The paper closes with a discussion of the results obtained in the study.

Governing Equations

The conservation equations of the two-dimensional Euler equations in generalized coordinates can be written as

$$\hat{Q}_t + \hat{E}_\xi + \hat{F}_\eta = 0 \tag{1}$$

where

$$\hat{Q} = Q/J \tag{2a}$$

$$\hat{E} = (\xi_x E + \xi_y F)/J \tag{2b}$$

$$\hat{F} = (\eta_x E + \eta_y F)/J \tag{2c}$$

and where the metric Jacobian is

$$J = \xi_x \eta_y - \xi_y \eta_x \tag{2d}$$

Received June 16, 1994; revision received Jan. 30, 1995; accepted for publication Jan. 30, 1995.

*Research Scholar, Department of Mechanical Engineering.
†Professor, Department of Mechanical Engineering.
‡Assistant Professor, Department of Aerospace Engineering.

In Cartesian coordinates the conservative vector is given by

$$Q = [\rho, \rho u, \rho v, e_t]^T \tag{3a}$$

$$E = \left[\rho u, (\rho u^2 + p), \rho uv, (e_t + p)u\right]^T \tag{3b}$$

$$F = \left[\rho v, \rho uv, (\rho v^2 + p), (e_t + p)v\right]^T \tag{3c}$$

For an ideal gas the pressure is related to γ, ρ, u, v and e_t as

$$p = (\gamma - 1)\left[e_t - 0.5\rho(u^2 + v^2)\right] \tag{3d}$$

Equation (1) is a hyperbolic system of conservation laws, hence, both hyperbolicity and conservation law properties can be utilized to construct the solution procedure. In particular, in this paper the given properties are invoked in the construction of the dissipation terms.

Description of the Algorithm

First, the computational mesh (ξ_j, η_k) is defined, with the mesh size $\Delta\xi$ and $\Delta\eta$. Let $Q^n_{j,k}$ denote the value of Q at time $n\Delta t$ and at the position $(j\Delta\xi, k\Delta\eta)$.

MacCormack Predictor–Corrector Scheme

The predictor step is

$$\hat{Q}^{(1)}_{j,k} = \hat{Q}^n_{j,k} - \frac{\Delta t}{\Delta\xi}\left(\hat{E}^n_{j+1,k} - \hat{E}^n_{j,k}\right) - \frac{\Delta t}{\Delta\eta}\left(\hat{F}^n_{j,k+1} - \hat{F}^n_{j,k}\right) \tag{4a}$$

The corrector step is

$$\hat{Q}^{(2)}_{j,k} = 0.5\left[\hat{Q}^n_{j,k} + \hat{Q}^{(1)}_{j,k} - \frac{\Delta t}{\Delta\xi}\left(\hat{E}^{(1)}_{j,k} - \hat{E}^{(1)}_{j-1,k}\right) - \frac{\Delta t}{\Delta\eta}\left(\hat{F}^{(1)}_{j,k} - \hat{F}^{(1)}_{j,k-1}\right)\right] \tag{4b}$$

$$\hat{Q}^{n+1}_{j,k} = \hat{Q}^{(2)}_{j,k} \begin{array}{l} +0.5\left[(R\Phi/J)^{(2)}_{j+\frac{1}{2},k} - (R\Phi/J)^{(2)}_{j-\frac{1}{2},k}\right] \\ +0.5\left[(R\Phi/J)^{(2)}_{j,k+\frac{1}{2}} - (R\Phi/J)^{(2)}_{j,k-\frac{1}{2}}\right] \end{array} \tag{4c}$$

Since the MacCormack scheme combines the forward and backward differences in separate predictor and corrector steps, four different schemes can be defined using the various combinations of one sided differences. In the present investigation, each of these four possibilities is employed in a cyclic fashion to avoid a bias provided by an eventual accumulation of errors.

Operator Splitting due to Strang

By employing Strang-type dimensional splitting, the solution procedure becomes locally one dimensional:

$$\hat{Q}^{n+2} = L_\xi(\Delta t)L_\eta(\Delta t)L_\eta(\Delta t)L_\xi(\Delta t)\hat{Q}^n \tag{5a}$$

where

$$L_\xi(\Delta t)\hat{Q}^n = \hat{Q}^* \tag{5b}$$

$$\hat{Q}^* = \hat{Q}^n - \frac{\Delta t}{\Delta\xi}\left[\tilde{E}^n_{j+\frac{1}{2},k} - \tilde{E}^n_{j-\frac{1}{2},k}\right] \tag{5c}$$

$$L_\eta(\Delta t)\hat{Q}^* = \hat{Q}^* - \frac{\Delta t}{\Delta\eta}\left[\tilde{F}^*_{j,k+\frac{1}{2}} - \tilde{F}^*_{j,k-\frac{1}{2}}\right] \tag{5d}$$

Typically,

$$\tilde{E}^n_{j+\frac{1}{2},k} = 0.5\begin{bmatrix} (\xi_x/J)_{j+\frac{1}{2},k}\left[E^n_{j,k} + E^n_{j+1,k}\right] \\ +(R\Phi/J)^n_{j+\frac{1}{2},k} \\ +(\xi_y/J)_{j+\frac{1}{2},k}\left[F^n_{j,k} + F^n_{j+1,k}\right] \end{bmatrix} \tag{5e}$$

In the preceding definition

$$(\xi_x/J)_{j+\frac{1}{2},k} = 0.5[(\xi_x/J)_{j+1,k} + (\xi_x/J)_{j,k}] \tag{6a}$$

$$(\xi_y/J)_{j+\frac{1}{2},k} = 0.5[(\xi_y/J)_{j+1,k} + (\xi_y/J)_{j,k}] \tag{6b}$$

$$(1/J)_{j+\frac{1}{2},k} = 0.5[(1/J)_{j+1,k} + (1/J)_{j,k}] \tag{6c}$$

Beam and Warming Implicit Scheme

$$\hat{Q}^{n+1}_{j,k} + \frac{\Delta t}{\Delta\xi}\left[\tilde{E}^{n+1}_{j+\frac{1}{2},k} - \tilde{E}^{n+1}_{j-\frac{1}{2},k}\right] + \frac{\Delta t}{\Delta\eta}\left[\tilde{F}^{n+1}_{j,k+\frac{1}{2}} - \tilde{F}^{n+1}_{j,k-\frac{1}{2}}\right] = \text{RHS} \tag{7a}$$

$$\text{RHS} = \hat{Q}^n_{j,k} + \frac{\Delta t}{\Delta\xi}\left[\tilde{E}^n_{j+\frac{1}{2},k} - \tilde{E}^n_{j-\frac{1}{2},k}\right] + \frac{\Delta t}{\Delta\eta}\left[\tilde{F}^n_{j,k+\frac{1}{2}} - \tilde{F}^n_{j,k-\frac{1}{2}}\right] \tag{7b}$$

In Eqs. (7) $E^n_{j+1/2,k}$ is given by Eq. (5e). In the present investigation a conservative Linearized alternating direction implicit (ADI) form[15] of Eq. (7) is used:

$$\text{RHS1} = -\frac{\Delta t}{\Delta\xi}\left[\tilde{E}^n_{j+\frac{1}{2},k} - \tilde{E}^n_{j-\frac{1}{2},k}\right] - \frac{\Delta t}{\Delta\eta}\left[\tilde{F}^n_{j,k+\frac{1}{2}} - \tilde{F}^n_{j,k-\frac{1}{2}}\right] \tag{8a}$$

$$\left[I + \frac{\Delta t}{\Delta\xi}H^\xi_{j+\frac{1}{2},k} - \frac{\Delta t}{\Delta\xi}H^\xi_{j-\frac{1}{2},k}\right]\Delta Q^* = \text{RHS1} \tag{8b}$$

$$\left[I + \frac{\Delta t}{\Delta\eta}H^\eta_{j,k+\frac{1}{2}} - \frac{\Delta t}{\Delta\eta}H^\eta_{j,k-\frac{1}{2}}\right]\Delta Q = \Delta Q^* \tag{8c}$$

$$\hat{Q}^{n+1}_{j,k} = \hat{Q}^n_{j,k} + \Delta Q \tag{8d}$$

where

$$H^\xi_{j+\frac{1}{2},k}\Delta Q^* = 0.5\left[\hat{A}_{j+1,k}\Delta Q^*_{j+1,k} - \Omega_{j+\frac{1}{2},k}\left(\Delta Q^*_{j+1,k} - \Delta Q^*_{j,k}\right) + \hat{A}_{j,k}\Delta Q^*_{j,k}\right] \tag{8e}$$

and

$$\hat{A}_{j+1,k} = \left[(\xi_x/J)_{j+\frac{1}{2},k}A_{j+1,k} + (\xi_y/J)_{j+\frac{1}{2},k}B_{j+1,k}\right] \tag{8f}$$

$$\hat{A}_{j,k} = \left[(\xi_x/J)_{j+\frac{1}{2},k}A_{j,k} + (\xi_y/J)_{j+\frac{1}{2},k}B_{j,k}\right] \tag{8g}$$

$$A = \frac{\partial E}{\partial Q} \quad \text{and} \quad B = \frac{\partial F}{\partial Q} \tag{9}$$

The term Ω will be explained in conjunction with dissipation.

Description of Dissipation

Since the system of governing equations is hyperbolic, a real and distinct set of eigenvectors must exist. The eigenvector matrix for $\delta E/\delta Q$ is evaluated at some symmetric average of $Q_{j,k}$ and $Q_{j+1,k}$, for example Roe's average,[16] where

$$D = (\rho_{j+1,k}/\rho_{j,k})^{\frac{1}{2}} \tag{10a}$$

$$u_{j+\frac{1}{2},k} = (Du_{j+1,k} + u_{j,k})/(D+1) \tag{10b}$$

$$v_{j+\frac{1}{2},k} = (Dv_{j+1,k} + v_{j,k})/(D+1) \tag{10c}$$

$$h_{j+\frac{1}{2},k} = (Dh_{j+1,k} + h_{j,k})/(D+1) \tag{10d}$$

$$c^2_{j+\frac{1}{2},k} = (\gamma - 1)[h - 0.5(u^2 + v^2)]_{j+\frac{1}{2},k} \tag{10e}$$

In addition, in the evaluation of the eigenvector matrix, the following are required:

$$k_1 = (\xi_x/J)_{j+\frac{1}{2},k} \Big/ \left[(\xi_x/J)^2_{j+\frac{1}{2},k} + (\xi_y/J)^2_{j+\frac{1}{2},k}\right]^{\frac{1}{2}} \quad (11a)$$

$$k_2 = (\xi_y/J)_{j+\frac{1}{2},k} \Big/ \left[(\xi_x/J)^2_{j+\frac{1}{2},k} + (\xi_y/J)^2_{j+\frac{1}{2},k}\right]^{\frac{1}{2}} \quad (11b)$$

The $\Phi_{j+1/2,k}$ can be divided into two types. 1) A spatially second-order symmetric TVD type scheme in which the numerical dissipation is independent of the sign of the characteristic speed. 2) A spatially second-order upwind TVD type scheme in which the numerical dissipation depends on the sign of the characteristic speed.

The elements of $\Phi_{j+1/2,k}$ in the ξ direction are given by $\phi^m_{j+1/2,k}$. For a symmetric TVD scheme

$$\phi^m_{j+\frac{1}{2},k} = \psi\left(a^m_{j+\frac{1}{2},k}\right)\left[\alpha^m_{j+\frac{1}{2},k} - \beta^m_{j+\frac{1}{2},k}\right] \quad (12)$$

The eigenvalues (characteristic speed) of the matrix $\delta E/\delta Q$ evaluated at the symmetric average of $Q_{j,k}$ and $Q_{j+1,k}$ are

$$(\bar{U}+\bar{c})_{j+\frac{1}{2},k}, \quad \bar{U}_{j+\frac{1}{2},k}, \quad (\bar{U}-\bar{c})_{j+\frac{1}{2},k}, \quad \bar{U}_{j+\frac{1}{2},k} \quad (13)$$

with

$$\bar{U}_{j+\frac{1}{2},k} = (\xi_x u + \xi_y v)_{j+\frac{1}{2},k} \quad (14a)$$

$$\bar{c}_{j+\frac{1}{2},k} = c_{j+\frac{1}{2},k}\left[\left(\xi_x^2 + \xi_y^2\right)_{j+\frac{1}{2},k}\right]^{\frac{1}{2}} \quad (14b)$$

The function ψ is given as

$$\psi(z) = \begin{cases} |z| & |z| \geq \delta \\ 0.5(z^2/\delta + \delta) & |z| < \delta \end{cases} \quad (15a)$$

where δ is a small positive parameter given as

$$\delta = \tilde{\delta}[|\bar{U}| + |\bar{V}| + C]_{j+\frac{1}{2},k} \quad \text{and} \quad \tilde{\delta} \approx 0.05 \quad (15b)$$

$$C_{j+\frac{1}{2},k} = 0.5c_{j+\frac{1}{2},k}\left[\left(\xi_x^2+\xi_y^2\right)^{\frac{1}{2}} + \left(\eta_x^2+\eta_y^2\right)^{\frac{1}{2}}\right]_{j+\frac{1}{2},k} \quad (15c)$$

The limiter employed in the present study is

$$\beta^m_{j+\frac{1}{2},k} = \text{minmod}\left(\alpha^m_{j+\frac{1}{2},k}, \alpha^m_{j-\frac{1}{2},k}\right) + \text{minmod}\left(\alpha^m_{j+\frac{1}{2},k}, \alpha^m_{j+\frac{3}{2},k}\right) - \alpha^m_{j+\frac{1}{2},k} \quad (16a)$$

in which

$$\alpha^l_{j+\frac{1}{2},k} = R^{-1}_{j+\frac{1}{2},k}(Q_{j+1,k} - Q_{j,k}) \quad (16b)$$

$$\text{minmod}(x,y) = \text{sign}(x)\begin{cases} \min(|x|,|y|) & x\cdot y > 0 \\ 0 & x \cdot y \leq 0 \end{cases} \quad (16c)$$

The elements of Φ can be upwind weighted if

$$\phi^m_{j+\frac{1}{2},k} = 0.5\psi\left(a^m_{j+\frac{1}{2},k}\right)\left(g^m_{j+1,k} + g^m_{j,k}\right) - \psi\left(a^m_{j+\frac{1}{2},k} + \gamma^m_{j+\frac{1}{2},k}\right)\alpha^m_{j+\frac{1}{2},k} \quad (17a)$$

where, in addition to the quantities explained in connection with the symmetric limiter,

$$g^m_{j,k} = \text{minmod}\left(\alpha^m_{j+\frac{1}{2},k}, \alpha^m_{j-\frac{1}{2},k}\right) \quad (17b)$$

$$\gamma^m_{j+\frac{1}{2},k} = 0.5\psi\left(a^m_{j+\frac{1}{2},k}\right) \times \begin{cases} \left(g^m_{j+1,k} - g^m_{j,k}\right)/\alpha^m_{j+\frac{1}{2},k} & \alpha^m_{j+\frac{1}{2},k} \neq 0 \\ 0 & \alpha^m_{j+\frac{1}{2},k} = 0 \end{cases} \quad (17c)$$

In the case of the implicit scheme there is a contribution of TVD dissipation to the implicit operator. It is given by

$$\Omega_{j+\frac{1}{2},k} = R_{j+\frac{1}{2},k}\text{diag}\left[\psi\left(a_{j+\frac{1}{2},k}\right)\right]R^{-1}_{j+\frac{1}{2},k} \quad (18)$$

Initial and Boundary Conditions

Initial Conditions

The problem is a circular cylinder of unit diameter placed in a hypersonic stream (Mach number = 15). The mesh chosen is such that there are 61 points in the tangential direction and 31 points in the radial direction. The inflow boundary values are taken to be freestream values. The value of pressure at the wall is obtained from the modified Newtonian expression[17]

$$p_w = (p_0 - p_{\text{fs}})\cos^2\theta + p_{\text{fs}} \quad (19)$$

A distribution of tangential velocity is first assumed (radial velocity is set to zero as it should be), satisfying the condition that the tangential velocity must be zero at the stagnation point. The velocity at the outer boundary point is assumed to be the freestream velocity to start with. The values of the components of velocity u and v are obtained therefrom by a simple transformation. Having obtained u, v, and p from Eq. (19), the density is obtained by invoking the fact that the stagnation enthalpy remains constant. The flow variables ρ, u, v, and p are then interpolated between the wall and the freestream.

Boundary Conditions

Since the flow is supersonic, all of the four variables are prescribed at the inflow boundary. The outflow also being supersonic, the variables are extrapolated from the interior. In the present method zeroth-order extrapolation is employed.

Tangency is imposed on the wall, i.e.,

$$\bar{V} = 0 \quad (20)$$

The pressure is obtained from the normal momentum equation

$$\left(\eta_x^2+\eta_y^2\right)p_\eta + (\xi_x\eta_x + \xi_y\eta_y)p_\xi = -\rho\bar{U}(\xi_x u_\xi + \xi_y v_\xi) \quad (21)$$

The temperature is obtained by imposing the adiabatic wall condition

$$\left(\eta_x^2+\eta_y^2\right)T_\eta + (\xi_x\eta_x + \xi_y\eta_y)T_\xi = 0 \quad (22)$$

The density is obtained from the ideal gas equation of state

$$\rho = p/RT \quad (23)$$

It may be observed that, in addition to the boundary conditions for the variables, the limiters also require some kind of boundary application.

Both with upwind and symmetric limiters, the respective limiters are extrapolated from the interior using zeroth-order extrapolation. However, in the case of a symmetric limiter it must be ensured that

$$\text{sign}(\alpha) = \text{sign}(\alpha - \beta) \quad (24)$$

It was found from trial runs that if the condition is not met, the scheme becomes unstable. The time step chosen is determined from the Courant–Fredrichs–Lewy (CFL) criterion.

Results and Discussion

The schemes just described were programmed and run on a PC486. Typical results from the extensive runs conducted are reported here.

1) Scheme A is the MacCormack scheme with a symmetric limiter and a CFL of 0.5.

2) Scheme B is the operator split scheme with an upwind limiter and a CFL of 0.05.

3) Scheme C is the same as scheme 2 but with a variable CFL with an initial CFL of 0.5 and a final CFL of 0.05.

4) Scheme D is the implicit scheme with variable CFL. Since the initial guess is quite different from the final solution, for the implicit

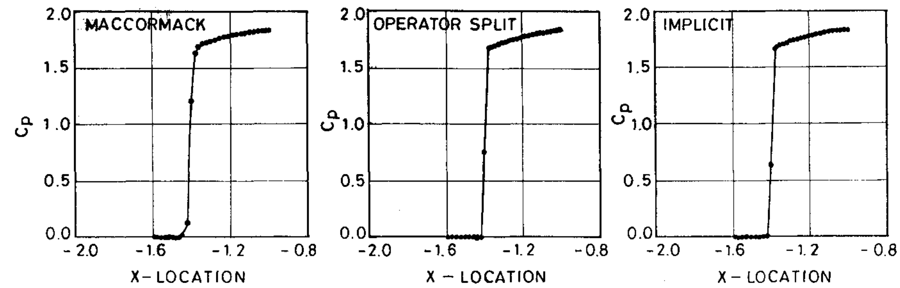

Fig. 1 Comparison of entropy.

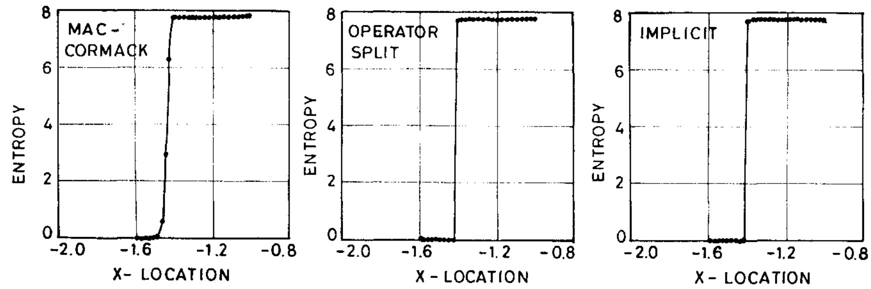

Fig. 2 Comparison of nondimensional pressure coefficient.

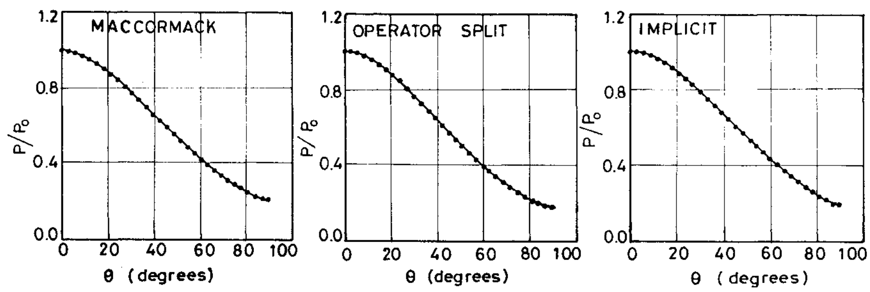

Fig. 3 Comparison of wall pressure distribution.

scheme a slow start up from the initial conditions was necessary. This was done by using a lower CFL at the start and progressively increasing it later. The results shown are for an initial CFL of 0.5 and a final CFL of 4.5.

5) A combination of operator split scheme and implicit scheme was also run. In this run the operator split scheme with a CFL of 0.5 was run up to 2000 time steps, and then the implicit scheme with a CFL of 4.5 was run. The advantage of this combination (E) is that it provides a better guess for the implicit scheme than in scheme D. Although the combination scheme required two different schemes it was observed to have some advantages.

Figures 1 and 2 show the plots of nondimensional pressure coefficient and entropy along the midplane for the three schemes, respectively. Figure 3 shows the pressure distribution on the wall and Fig. 4 the Mach contours.

From Figs. 1 and 2, it can be seen that the various schemes capture shocks in 2–3 mesh points. Also, as with TVD schemes, there are no oscillations in the vicinity of shocks. The MacCormack scheme is slightly diffusive. This is because the symmetric limiter was used. This conclusion was substantiated by a run conducted using the symmetric limiter with the operator split scheme. The computed pressure distribution is shown in Fig. 3. It agrees well with the results computed using the modified-Newtonian expression.

Table 1 shows the CPU times for the various runs. From the table it can be concluded that the combination scheme is the quickest. The implicit scheme D comes next followed by the explicit schemes. Among the explicit schemes, the MacCormack scheme is faster than the operator split with 0.05 CFL. However, the operator split scheme with a variable CFL falls between the MacCormack and the implicit scheme.

Figure 5 shows the plot of residuals for the various schemes. It can be seen from the figure that the combination scheme E and the implicit scheme D converge to machine accuracy in about 3000 time steps. The explicit schemes converge to higher residuals in about 20,000 time steps. For the operator split scheme, an interesting observation is that reduction of CFL from 0.5 to 0.05 after 2000 time steps (C) results in faster convergence; the solution converges in about 10,000 time steps. The convergence of the operator split scheme for fixed CFL is better in comparison to the MacCormack scheme.

Table 1 Comparison of CPU times for various runs

Scheme	Run	CFL	CPU, s
A	MacCormack	0.5	500
B	Operator split	0.05	650
C	Operator split	Variable	325
D	Implicit	Variable	240
E	Combination	Variable	150

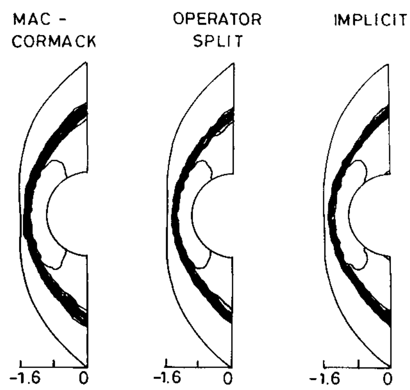

Fig. 4 Plot of Mach contours.

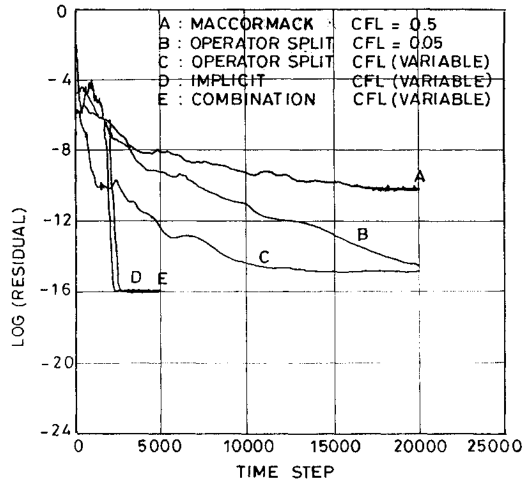

Fig. 5 Plot of convergence history.

Conclusions

All of the schemes considered here produce sharp resolution of the shocks. In general, upwind dissipation produces better resolution. As regards the quality of solution, all of the schemes are equally good. However, in terms of computational time, the combination scheme is the best followed by the implicit scheme. Between the explicit schemes the MacCormack scheme is faster. From the standpoint of convergence, the combination scheme and the implicit scheme are equally good. The explicit schemes converge to higher residuals and between them a variable CFL operator split scheme is satisfactory.

References

[1]Biringen, S., and McMillan, O. J., "The Implicit Method for the Calculation of Inlet Flow Fields," NASA CR-3413, June 1981.

[2]Yee, H. C., "A Class of High Resolution Explicit and Implicit Shock Capturing Method," NASA TM-101088, Feb. 1989.

[3]Harten, A., "A High Resolution Scheme for the Computation of Weak Solution of Hyperbolic Conservation Laws," *Journal of Computational Physics*, Vol. 49, 1983, pp. 357–393.

[4]Yee, H. C., "Construction of Explicit and Implicit Symmetric TVD Schemes and Their Applications," *Journal of Computational Physics*, Vol. 68, 1987, pp. 151–179.

[5]Boris, J. P., and Book, D. L., "Flux Corrected Transport-I SHASTA. A Fluid Transport Algorithm that Works," *Journal of Computational Physics*, Vol. 11, 1973, pp. 38–69.

[6]Collela, P., and Woodward, P. R., "The Piecewise Parabolic Method (PPM) for Gasdynamic Simulation," *Journal of Computational Physics*, Vol. 54, 1984, pp. 174–201.

[7]Harten, A., "On the Class of High Resolution Total Variation Stable Finite Difference Scheme," *SIAM Journal of Numerical Analysis*, Vol. 21, 1984, pp. 1–23.

[8]Sweby, P. K., "High Resolution Schemes Using Flux Limiters for Hyperbolic Conservation Laws," *SIAM Journal of Numerical Analysis*, Vol. 21, 1984, pp. 995–1011.

[9]Montagne, J. L., Yee, H. C., and Vinokur, M., "Comparative Study of High Resolution Shock Capturing Schemes for Real Gases," NASA TM-86839, July 1987.

[10]Yang, H. Q., and Przekwas, J., "A Comparative Study of Advanced Shock Capturing Schemes Applied Burger Equation," *Journal of Computational Physics*, Vol. 102, 1992, pp. 139–159.

[11]Woodward, P. L., and Collela, P., "The Numerical Simulation of Two-Dimensional Fluid Flow with Strong Shocks," *Journal of Computational Physics*, Vol. 51, 1984, pp. 115–174.

[12]MacCormack, R. W., "The Effect of Viscosity in Hypervelocity Impact Cratering," AIAA Paper 69–0354, 1969.

[13]Strang, G., "On the Construction and Comparison of Difference Schemes," *SIAM Journal of Numerical Analysis*, Vol. 5, 1968, pp. 506–517.

[14]Beam, R. M., and Warming, R. F., "An Implicit Finite Difference Algorithm for Hyperbolic System in Conservation Law Form," *Journal of Computational Physics*, Vol. 22, 1976, pp. 87–110.

[15]Yee, H. C., "Linearised Form of Implicit TVD Schemes for Multi-Dimensional Euler and Navier–Stokes Equations," *Computers and Mathematics with Applications*, Vol. 12A, 1986, pp. 413–432.

[16]Roe, P. L., "Approximate Riemann Solvers, Parameter Vectors, and Difference Schemes," *Journal of Computational Physics*, Vol. 43, 1981, pp. 357–372.

[17]Tannehill, J. C., Holst, T. L., and Rakich, J. V., "Numerical Computation of Two-Dimensional Viscous Blunt Body Flows with an Impinging Shock," *AIAA Journal*, Vol. 14, 1976, pp. 204–211.